

Extended Strip Model for Slabs Subjected to a Combination of Loads

Lantsoght, Eva; van der Veen, Cor; de Boer, A.

DOI

[10.1007/978-3-319-59471-2_76](https://doi.org/10.1007/978-3-319-59471-2_76)

Publication date

2018

Document Version

Final published version

Published in

High Tech Concrete: Where Technology and Engineering Meet

Citation (APA)

Lantsoght, E., van der Veen, C., & de Boer, A. (2018). Extended Strip Model for Slabs Subjected to a Combination of Loads. In D. Hordijk, & M. Lukovic (Eds.), *High Tech Concrete: Where Technology and Engineering Meet: Proceedings of the 2017 fib Symposium, held in Maastricht, The Netherlands, June 12–14, 2017* (pp. 641-649) https://doi.org/10.1007/978-3-319-59471-2_76

Important note

To cite this publication, please use the final published version (if applicable).
Please check the document version above.

Copyright

Other than for strictly personal use, it is not permitted to download, forward or distribute the text or part of it, without the consent of the author(s) and/or copyright holder(s), unless the work is under an open content license such as Creative Commons.

Takedown policy

Please contact us and provide details if you believe this document breaches copyrights.
We will remove access to the work immediately and investigate your claim.

Extended Strip Model for Slabs Subjected to a Combination of Loads

Eva O.L. Lantsoght^{1,2(✉)}, Cor van der Veen¹, and Ane de Boer³

¹ Concrete Structures, Delft University of Technology,
Stevinweg 1, 2628 Delft, The Netherlands

{E. O. L. Lantsoght, C. vanderveen}@tudelft.nl

² Politecnico, Universidad San Francisco de Quito,
Diego de Robles Y Pampite, Cumbaya, Quito, Ecuador
elantsoght@usfq.edu.ec

³ Rijkswaterstaat, Ministry of Infrastructure and the Environment,
24057, 2502 Utrecht, The Netherlands
ane.de.boer@rws.nl

Abstract. Reinforced concrete slab bridges are assessed for a combination of loads that include self-weight, superimposed loads, and distributed and concentrated live loads. The shear capacity of reinforced concrete slabs subjected to a combination of loads is thus an important topic for the assessment of existing bridges. Currently, a plastic model exists for the assessment of reinforced concrete solid slabs subjected to a concentrated load: the Extended Strip Model, based on the Strip Model for concentric punching shear. To apply this model to slabs subjected to a combination of loads, the model needs to be adapted based on theoretical principles. The results are then compared with the results from experiments on half-scale slab bridges subjected to a combination of a concentrated load close to the support and a line load. The result of this comparison is that the proposed method is suitable to find a safe estimate of the maximum concentrated load on the slab. The implication of this development is that an improved tool is available to estimate the maximum load of a truck that can be placed on a reinforced concrete bridge, thus improving the current assessment.

Keywords: Experiments · Extended strip model · Punching · Shear · Slabs

1 Introduction

Since the bridge stock in Europe and North America is aging, it is important to develop methods that are suitable for the assessment of existing bridges. In the Netherlands, a good share of the bridge stock consists of reinforced concrete solid slab bridges, mostly built during the 1960s and 1970s (Lantsoght et al. 2013a). The prescribed live load model is a combination of distributed lane loads and concentrated loads (design tandem). When the recently implemented Eurocodes are used for the assessment of these bridges, they tend to not fulfill the requirements for shear. Experiments (Lantsoght et al. 2013b) have shown that slabs under concentrated loads have larger shear capacities than beams as a result of transverse load distribution in slabs. A slab develops a two-dimensional load path, whereas the load path in a beam is one-dimensional. When one-way slabs under concentrated loads are tested to failure, their behavior is a

complex combination of one-way shear, two-way shear, and flexure. The traditional one-way shear methods are thus not suitable for application to slabs. Additionally, methods for the assessment of slab bridges under live loads should be able to deal with the complex load combination of distributed and concentrated loads.

2 Extended Strip Model

Extended Strip Model for slabs under a single concentrated load. The Extended Strip Model is derived from the Strip Model for concentric punching shear in slabs (Alexander and Simmonds 1992; Ospina et al. 2003; Afhami 1997). The Strip Model is a lower-bound plasticity-based model, in line with the Strip Method for flexure (Hillerborg 1975), and describes a load path prior to failure. This load path consists of strips, working in arching action (one-way shear), and quadrants working in two-way flexure, see Fig. 1a. Failure is described at the breakdown of this load path, by achieving the maximum one-way shear (represented by the inclined cracking load) at the interface between the strip and quadrant. The Extended Strip Model (Lantsoght et al. (in press); Lantsoght et al. 2016) applies these concepts to one-way slabs under concentrated loads to describe the complex combination of one-way shear, two-way shear, and flexure that governs this case. For this case, the geometry, the bending moment and shear diagrams, and the effect of torsion need to be considered, see Fig. 1b. Where the limiting shear acting on the intersection between the quadrants and strips is uniform for the Strip Model, it is influenced by the previously mentioned parameters in the Extended Strip Model.

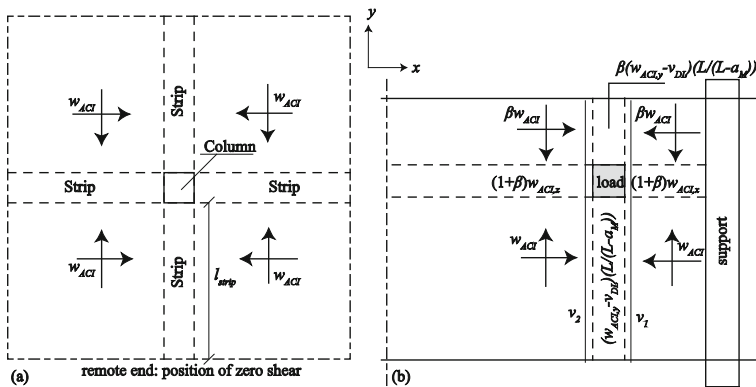


Fig. 1. (a) Strip Model and (b) Extended Strip Model

The effect of torsion was derived based on linear finite element studies (Valdivieso et al. 2016), and simplified into the expression:

$$\beta = 0.8 \frac{a}{d_x} \frac{b_r}{b} \text{ for } 0 \leq \frac{a}{d_x} \leq 2.5 \text{ and } 0 \leq \frac{b_r}{b} \leq \frac{1}{2} \quad (1)$$

with a the shear span, d_x the effective depth to the longitudinal reinforcement, b_r the distance between the load and the edge, and b the full slab width. For $a/d_x > 2.5$, the value of a/d_x in Eq. (1) is replaced by 2.5. The geometry is taken into account by considering the compressive strut that forms between the load and the support for loads close to the support, and by comparing the physical strip length of the strip between the load and the edge l_{edge} to the loaded length l_w assumed in the model. The bending moment diagram is taken into account by L , the distance between the points of inflection, and a_M , the distance between the load and the nearest position of zero moment. The shear diagram is taken into account by looking at v_1 and v_2 , the shear force left and right of the load. The load-carrying mechanism will break down when the largest of these two shear forces reaches the inclined cracking load w_{ACI} . The effect of the self-weight is added through v_{DL} .

Extended Strip Model for slabs subjected to a combination of loads. For slabs subjected to a combination of loads, the Extended Strip Model can be used as well. When a combination of concentrated loads is used, as for example for the case of the design tandem from the code, the perimeter of these loads can be used to activate the strips and quadrants. An application of such a combination of loads was used to determine the maximum load on the Ruytenschildt Bridge (Lantsoght et al. 2016), where the Extended Strip Model resulted in a safe lower bound. For slabs under a combination of distributed and concentrated loads, such as live load models, the effect of the distributed loads can be taken into account on the strips in the transverse direction. In Fig. 2 the effect of the distributed loads is represented by v_{dist} , the shear force at the position of the concentrated load caused by the distributed load. The resulting maximum load according to the Extended Strip Model is:

$$P_{ESM} = P_x + P_{sup} + P_y + P_{edge} \quad (2)$$

$$P_x = \sqrt{2(1 + \beta)M_{sag,x}w_{ACI,x}} \quad (3)$$

$$P_{sup} = \frac{2d_x}{a_v} \sqrt{2(1 + \beta)M_{s,x}w_{ACI,x}} \quad (4)$$

$$P_y = \sqrt{2 \left(\frac{L}{L - a_M} \right) M_{s,y} (w_{ACI,y} - v_{DL} - v_{dist})} \quad (5)$$

$$P_{edge} = \begin{cases} \sqrt{2\beta \left(\frac{L}{L - a_M} \right) M_{s,y} (w_{ACI,y} - v_{DL} - v_{dist})} & \text{for } l_w < l_{edge} \\ \beta \left(\frac{L}{L - a_M} \right) (w_{ACI,y} - v_{DL} - v_{dist}) l_{edge} & \text{for } l_w \geq l_{edge} \end{cases} \quad (6)$$

In Eq. (2), P_x is the capacity of a strip in the longitudinal direction, P_{sup} the capacity of a strip between the load and the support, provided that $2d_x/a_v \geq 1$, (otherwise $2d_x/a_v$ is replaced by 1), P_y the capacity of a strip in the transverse direction, and P_{edge} the

capacity of a strip between the load and the free edge in the transverse direction. $M_{sag,x}$, $M_{sag,y}$, $M_{hog,x}$ and $M_{hog,y}$ are respectively the sagging and hogging moment capacities in the x -direction (longitudinal) and y -direction (transverse), which are used to determine the bending moment capacities $M_{s,x}$ and $M_{s,y}$ used in Eqs. (4), (5) and (6), with:

$$M_{s,x} = M_{sag,x} + \lambda_{moment} M_{hog,x} \tag{7}$$

$$M_{s,y} = M_{sag,y} + \lambda_{moment} M_{hog,y} \tag{8}$$

with $\lambda_{moment} = M_{sup}/M_{span}$ with M_{sup} and M_{span} the support and span moments from the bending moment diagram respectively. The one-way shear capacity is defined as:

$$w_{ACI,x} = 0.166d_y \sqrt{f_{ck}} \left(\frac{100\text{mm}}{d} \right)^{\frac{1}{3}} \tag{9}$$

$$w_{ACI,y} = 0.166d_x \sqrt{f_{ck}} \left(\frac{100\text{mm}}{d} \right)^{\frac{1}{3}} \tag{10}$$

with f_{ck} the concrete cylinder compressive strength in [MPa], d_x the effective depth to the longitudinal reinforcement, d_y the effective depth to the transverse reinforcement, and d the average of d_x and d_y . For the edge strip, l_{edge} is the distance between the free edge and the face of the load, and

$$l_w = \sqrt{\frac{2M_{s,y}}{\beta(w_{ACI,y} - v_{DL} - v_{dist}) \frac{L}{L-a_M}}} \tag{11}$$

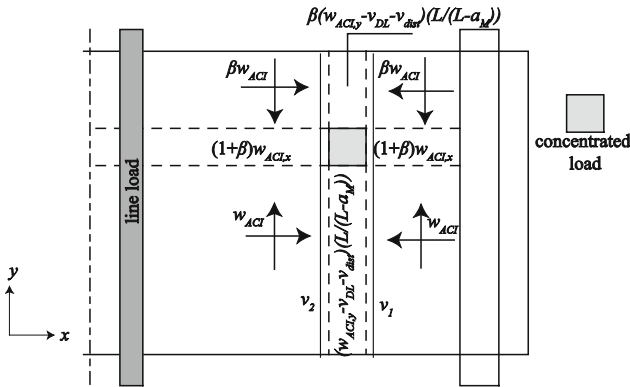


Fig. 2. Extended Strip Model for concentrated load and line load.

3 Experiments

Experimental setup. To study the effect of combined loads, a number of experiments were carried out in the Stevin II Laboratory of Delft University of Technology (Lantsoght et al. 2015). Eight slabs of $5\text{ m} \times 2.5\text{ m} \times 0.3\text{ m}$ were tested, resulting in 20 experiments. As live loads models prescribe the combination of a distributed lane load with design trucks or tandems, a simplified representation of this load combination was used by combining a concentrated load close to the support with a line load acting over the full slab width. The experiments were designed to have the contribution of the line load to the shear stress at the support as 50% of the failure shear stress at the support obtained from testing wide beams (Lantsoght et al. 2014). Therefore, a line load of 240 kN/m (600 kN on the jack) was chosen, applied at 1.2 m from the center of the support. This load was applied first and kept constant, after which the concentrated load, applied through a loading plate of $300\text{ mm} \times 300\text{ mm}$, was increased to failure. The test setup is shown in Fig. 3.

Materials. All slabs used ready-mix concrete C28/35 with a maximum aggregate size of 16 mm . The reinforcement bars were S500 steel with a measured yield strength of 542 MPa for the $\phi = 20\text{ mm}$ bars and 537 MPa for the $\phi = 10\text{ mm}$ bars.

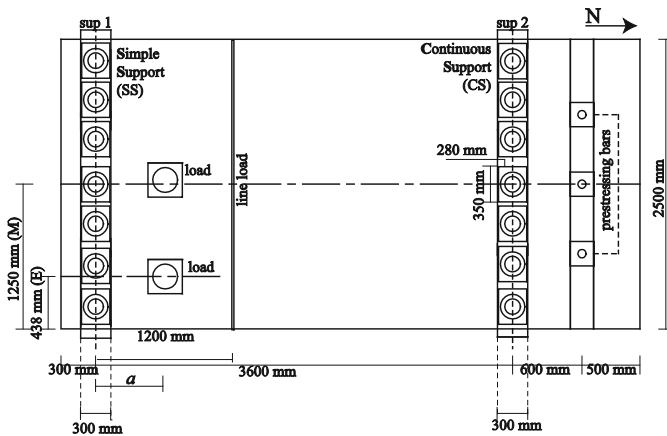


Fig. 3. Top view of test setup used to study slabs under a combination of loads.

4 Results

Failure load. An overview of the failure modes and maximum loads is given in Table 1. Table 1 shows the varied parameters: the experiment number, the support at which the experiment was carried out (simple support SS or continuous support CS), the span length l_{span} , the average cylinder compressive strength f_{cm} , the shear span a , the distance from the center of the load to the free edge b_r , and the width of the support. The results in Table 1 are the failure mode (B for beam shear, indicating a shear crack

at the side face, WB for wide beam shear, indicating inclined cracking on the bottom of the slab), the maximum concentrated load P_{conc} and the line load P_{line} . All other parameters were kept constant, except that for S20T2b a loading plate of 200 mm 200 mm was used.

Comparison between experiments and Extended Strip Model. The values of P_{conc} are then compared to the calculated values from the Extended Strip Model P_{ESM} from Eq. (2). The results of the calculations are summarized in Table 2, where λ is the ratio M_{sup}/M_{span} from the moment diagram at failure, and β , P_x , P_{sup} , P_y , l_w and P_{edge} are determined from Eqs. (1), (3), (4), (5), (6) and (11) respectively. The average value of P_{conc}/P_{ESM} is 1.47, with a coefficient of variation of 12.5% and a characteristic value (5% lower bound) of 1.17. These results show that the coefficient of variation is quite low for a shear problem with a complex loading situation that is tackled by a simple hand calculation. Moreover, as expected from a lower-bound plasticity-based approach, the calculated maximum loads are a safe lower bound of the experimentally obtained values.

Table 1. Overview of test results for slabs subjected to a combination of loads

Test		l_{span} (m)	f_{cm} (MPa)	a (m)	b_r (m)	b_{sup} (m)	Mode	P_{conc} (kN)	P_{line} (kN)
S20T1	SS	3.6	49.62	0.6	1.250	0.28	B	1542	603
S20T2b	CS	2.4	49.62	0.6	1.250	0.28	WB	1552	601
S20T3	CS	2.4	49.62	0.6	0.438	0.28	WB + B	1337	601
S20T4	CS	2.4	49.62	0.6	0.438	0.28	WB + B	1449	601
S21T1	CS	3.6	46.54	0.6	1.250	0.10	WB + B	1165	602
S21T2	SS	3.6	46.54	0.6	1.250	0.10	WB + B	1386	603
S22T1	CS	3.6	47.54	0.6	0.438	0.10	WB + B	984	602
S22T2	CS	3.6	47.54	0.6	0.438	0.10	WB + B	961	602
S22T3	SS	3.6	47.54	0.6	0.438	0.10	WB + B	978	603
S22T4	SS	3.6	47.54	0.6	0.438	0.10	WB + B	895	604
S23T1	CS	3.6	48.27	0.6	1.250	0.28	WB + B	1386	601
S23T2	SS	3.6	48.27	0.6	1.250	0.28	WB + B	1132	602
S24T1	CS	3.6	48.27	0.6	0.438	0.28	WB + B	1358	601
S24T2	CS	3.6	48.27	0.6	0.438	0.28	WB + B	1182	601
S24T3	SS	3.6	48.27	0.6	0.438	0.28	WB + B	995	602
S24T4	SS	3.6	48.27	0.6	0.438	0.28	WB + B	784	602
S25T2	CS	3.6	48.03	0.4	1.250	0.10	WB + B	1620	601
S25T3	CS	3.6	48.03	0.4	0.438	0.10	WB + B	1563	602
S26T1	SS	3.6	48.03	0.42	0.438	0.10	WB + B	1448	602
S26T2	SS	3.6	48.03	0.42	0.438	0.10	B	1324	602
S26T3	CS	3.6	48.03	0.4	1.250	0.10	WB + B	1555	602
S26T4	CS	3.6	48.03	0.4	0.438	0.10	B	1363	602
S26T5	CS	3.6	48.03	0.4	0.438	0.10	WB + B	1451	602

Table 2. Comparison between experiments and Extended Strip Model

Test	P_{conc} (kN)	λ	β	P_x (kN)	P_{sup} (kN)	P_y (kN)	l_w m	P_{edge} (kN)	P_{ESM} (kN)	P_{conc}/P_{ESM}
S20T1	1542	0.00	0.91	294	503	61	0.877	58	917	1.682
S20T2b	1552	0.73	0.91	240	465	85	0.728	81	872	1.781
S20T3	1337	0.81	0.32	245	562	106	1.545	11	924	1.447
S20T4	1449	0.72	0.32	245	549	104	1.502	11	909	1.595
S21T1	1165	0.33	0.91	289	441	61	1.161	55	847	1.376
S21T2	1386	0.00	0.91	289	383	56	0.955	53	781	1.774
S22T1	984	0.37	0.32	242	375	64	1.949	5	685	1.436
S22T2	961	0.36	0.32	242	373	63	1.942	5	684	1.406
S22T3	978	0.00	0.32	242	320	57	1.582	6	625	1.565
S22T4	895	0.00	0.32	242	320	57	1.581	6	625	1.432
S23T1	1386	0.27	0.91	292	562	63	1.085	60	977	1.419
S23T2	1132	0.00	0.91	292	499	58	0.918	56	905	1.251
S24T1	1358	0.27	0.32	243	468	63	1.833	6	779	1.744
S24T2	1182	0.27	0.32	243	468	63	1.834	6	779	1.518
S24T3	995	0.00	0.32	243	415	58	1.553	6	722	1.378
S24T4	784	0.00	0.32	243	415	59	1.547	6	722	1.085
S25T2	1620	0.43	0.60	267	848	63	1.486	36	1215	1.333
S25T3	1563	0.43	0.21	232	736	63	2.512	3	1035	1.511
S26T1	1448	0.00	0.22	233	562	56	1.952	4	855	1.693
S26T2	1324	0.00	0.22	233	562	56	1.949	4	855	1.548
S26T3	1555	0.53	0.60	267	877	65	1.544	36	1245	1.249
S26T4	1363	0.62	0.21	232	783	67	2.685	3	1085	1.256
S26T5	1451	0.58	0.21	232	774	66	2.653	3	1076	1.349

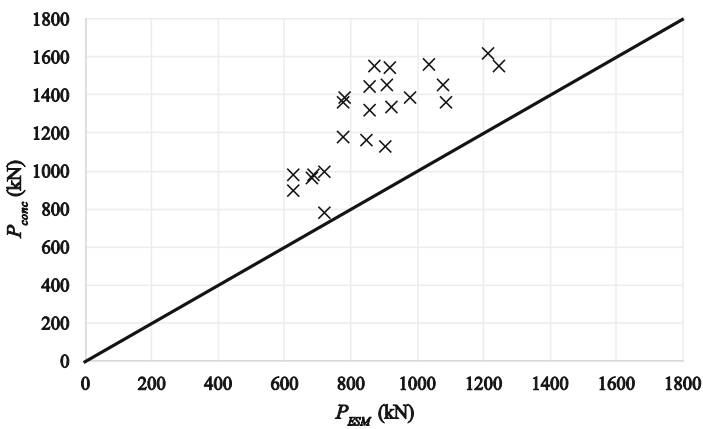


Fig. 4. Comparison between calculated and experimental results.

This result can also be observed from Fig. 4. It can be concluded that the proposed method is suitable for estimating the maximum concentrated load (design truck or tandem) that can be placed on a bridge, while taking into account the effect of the distributed loads. As such, the proposed method provides a simple and conservative tool for the first assessment of reinforced concrete slab bridges subjected to permanent loads and the live load model.

5 Summary and Conclusions

Reinforced concrete slab bridges subjected to the load combination of permanent loads and live loads, consisting of distributed lane loads and concentrated truck loads, present a complex case for shear assessment. Experiments have shown that one-way slabs under concentrated loads fail in a combination of one-way shear, two-way shear and flexure, and that the existing methods for one-way shear are overly conservative. Therefore, the Extended Strip Model was developed, which combines elements of one-way shear and two-way flexure. The original Extended Strip Model is suitable for finding the maximum concentrated load for a slab subjected to a single concentrated load. The model is now extended to find the maximum concentrated load for a slab subjected to a combination of loads. The proposed method is compared to the results from experiments on slabs under a combination of a line load over the width and a single concentrated load. This comparison shows that the proposed model leads to a good and safe prediction for the maximum concentrated load. As such, it can be used for a quick, first-order assessment of an existing reinforced concrete slab bridge subjected to a combination of distributed and concentrated loads.

Acknowledgments. The authors wish to express their gratitude and sincere appreciation to the Dutch Ministry of Infrastructure and the Environment (Rijkswaterstaat) for financing this research.

References

- Afhami, S.: Strip model for capacity of flat plate-column connections. Ph.D. Thesis, University of Alberta (1997)
- Alexander, S.D.B., Simmonds, S.H.: Bond model for concentric punching shear. *ACI Struct. J.* **89**(3), 325–334 (1992)
- Hillerborg, A.: Strip Method of Design. Viewpoint Publications, Cement and Concrete Association, Wexham Springs, Slough, England (1975)
- Lantsoght, E.O.L., van der Veen, C., de Boer, A., Alexander, S.: Bridging the gap between one-way and two-way shear in slabs. In: *ACI SP International Punching Symposium* (2016)
- Lantsoght, E.O.L., van der Veen, C., de Boer, A., Alexander, S.D.B.: Extended strip model for slabs under concentrated loads. *ACI Struct. J.* (in press)
- Lantsoght, E.O.L., van der Veen, C., De Boer, A., Walraven, J.: Influence of width on shear capacity of reinforced concrete members. *ACI Struct. J.* **111**(6), 1441–1450 (2014)

- Lantsoght, E.O.L., van der Veen, C., de Boer, A., Walraven, J.: One-way slabs subjected to combination of loads failing in shear. *ACI Struct. J.* **112**(4), 417–426 (2015)
- Lantsoght, E.O.L., van der Veen, C., de Boer, A., Walraven, J.C.: Recommendations for the shear assessment of reinforced concrete slab bridges from experiments. *Struct. Eng. Int.* **23**(4), 418–426 (2013a)
- Lantsoght, E.O.L., van der Veen, C., Walraven, J.C.: Shear in one-way slabs under a concentrated load close to the support. *ACI Struct. J.* **110**(2), 275–284 (2013b)
- Ospina, C.E., Alexander, S.D.B., Cheng, J.J.R.: Punching of two-way concrete slabs with fiber-reinforced polymer reinforcing bars or grids. *ACI Struct. J.* **100**(5), 589–598 (2003). doi:[10.14359/12800](https://doi.org/10.14359/12800)
- Valdivieso, D., Lantsoght, E.O.L., Sanchez, T.A.: Effect of torsion on shear capacity of slabs. In: SEMC 2016 symposium, Cape Town, South Africa (2016)